$LiNbO_3$ waveguides for integrated SPDC spectroscopy

Alexander S. Solntsev, Pawan Kumar, Thomas Pertsch, Andrey A. Sukhorukov, and Frank Setzpfandt

Citation: APL Photonics **3**, 021301 (2018); doi: 10.1063/1.5009766
View online: https://doi.org/10.1063/1.5009766
View Table of Contents: http://aip.scitation.org/toc/app/3/2
Published by the American Institute of Physics

$LiNbO_3$ waveguides for integrated SPDC spectroscopy

Alexander S. Solntsev,[1,2,a] Pawan Kumar,[3] Thomas Pertsch,[3]
Andrey A. Sukhorukov,[2] and Frank Setzpfandt[3,b]
[1]*School of Mathematical and Physical Sciences, University of Technology Sydney, Ultimo, NSW 2007, Australia*
[2]*Nonlinear Physics Centre, Research School of Physics and Engineering, Australian National University, Canberra, ACT 2601, Australia*
[3]*Institute of Applied Physics, Abbe Center of Photonics, Friedrich-Schiller-Universität Jena, Max-Wien-Platz 1, 07743 Jena, Germany*

(Received 19 October 2017; accepted 17 January 2018; published online 5 February 2018)

Spontaneous parametric down-conversion (SPDC) spectroscopy using photon pairs is a promising avenue towards affordable mid-infrared (MIR) spectroscopy. Here, we experimentally investigate the feasibility of using periodically poled waveguides in lithium niobate for SPDC spectroscopy applications. We find the waveguides suitable to generate wavelength non-degenerate photon pairs with one photon in the MIR spectral range with high fluence. We use this to determine the cutoff wavelengths of the waveguide mode in the MIR by performing only measurements in the near-infrared spectral range. https://doi.org/10.1063/1.5009766

Spectroscopy in the mid-infrared (MIR) spectral region is of great interest due to a variety of applications in biology, medicine, and chemistry.[1] The conventional direct approach to MIR spectroscopy requires light sources and detection detectors in that spectral range. Although quantum-cascade lasers as sources have become available in the last years, detectors suffer from low detection efficiency and strong noise due to black-body radiation and often have to be cooled to cryogenic temperatures. Nonlinear optics and light up-conversion can move at least the detection part of MIR spectroscopy into the much more accessible visible or near-infrared (NIR) spectral range.[2,3] However, due to their nonlinear nature, these techniques require high peak intensities and typically use multiple tunable pulsed lasers.

An alternative approach is spontaneous parametric down-conversion (SPDC) spectroscopy.[4,5] During the process of SPDC, short-wavelength pump photons are split into pairs of long-wavelength signal and idler photons, which can be generated in different wavelength ranges. The efficiency of this process depends on the material properties at all involved wavelengths. Hence, by analyzing only one of the photons, which can be detected classically, information about the properties of the system in the spectral range of the other photon can be extracted. This makes SPDC spectroscopy a powerful tool, especially for MIR measurements. The signal photon can be read out in the visible or NIR range, where the detection is simple and affordable, while the idler photon can probe the optical properties in the MIR range, which using conventional spectroscopic approaches would require expensive and bulky solutions. Furthermore, in contrast to other nonlinear spectroscopic approaches, only a single continuous-wave visible laser is required to generate sufficient photon numbers, allowing to perform measurements.

SPDC spectroscopy is based on the frequency correlations introduced by the down-conversion process, and therefore it can work in both the low gain regime, where the generated photon pairs do not act as seeds for more photon pairs, and the high gain regime, where this condition is violated. Traditionally, SPDC spectroscopy has been primarily used with low gain, although recently there has

[a]Electronic mail: Alexander.Solntsev@uts.edu.au
[b]Electronic mail: f.setzpfandt@uni-jena.de

been growing interest in developing high gain schemes.[6] SPDC spectroscopy has been utilized to measure the broadband refractive index dispersion[7,8] and the domain structure[9,10] of solids, as well as to precisely determine the optical properties of gases.[11] Recent progress allowed replacing the spectrometer with a camera and an interferometric scheme.[12] SPDC spectroscopy can also be useful in the THz frequency range.[13,14]

To date, all implementations of SPDC spectroscopy have utilized bulk optics, which suffers from large size, complex alignment, interferometric instability, and small effective nonlinearities. On-chip integration has the potential to solve these issues, and various on-chip platforms have been successfully used for SPDC.[15,16] In waveguides made from gallium arsenide, SPDC to signal and idler photons with strongly different wavelengths has been shown, and the spectral analysis of this process has been used to determine losses in the MIR spectral region covered by the idler photon.[17]

In this work, we demonstrate the feasibility of titanium-indiffused $LiNbO_3$ waveguides, a standard platform for many photonic applications,[18,19] as building blocks for SPDC spectroscopy on photonic chips. To this end, we demonstrate that strongly non-degenerate photon pairs with idler wavelengths can be generated with a tunable wavelength up to the MIR spectral region, similar to high-power parametric generation but using only a low-power continuous-wave (cw) pump laser.[19] We pump a periodically poled Ti-diffused $LiNbO_3$ waveguide of cw laser with a wavelength λ_p between 740 nm and 780 nm and a power of 0.5 mW. Photon pairs are generated in the waveguide through SPDC [Fig. 1(a)]. $LiNbO_3$ waveguides provide high field confinement and strong nonlinearity, which enables efficient SPDC even when pumped by a low-power cw laser.[20] SPDC in principle allows the generation of signal and idler photons with wavelengths λ_s and λ_i, respectively, across a broad wavelength band.[21] Due to energy conservation, the frequencies of the generated photons are related by $\omega_p = \omega_s + \omega_i$ [Fig. 1(b)], where $\omega_n = 2\pi c_0/\lambda_n$ with $n = [p, i, s]$ and the vacuum velocity of light c_0. However, due to the typically long interaction length in optical waveguides, the generation efficiency η is ruled by the phase mismatch

$$\Delta\beta = k_p\left(\lambda_p\right) - k_s\left(\lambda_s\right) - k_i\left(\lambda_i\right) + 2\pi/\Lambda \tag{1}$$

of the three interacting modes according to

$$\eta \propto \mathrm{sinc}^2\left(\frac{\Delta\beta L}{2\pi}\right). \tag{2}$$

Here, the $k_i\left(\lambda_i\right)$ are the propagation constants of the waveguide modes, Λ is the period of the periodic poling used to control the phase-matching wavelength, and L is the waveguide length. For a given pump wavelength, this dependency of the efficiency on the pump wavelength selects certain wavelength bands for the generated signal and idler photons, in which the spectral width scales with $1/L$. Thus, the pump wavelength can be used to tune the signal and idler wavelengths, whereas the

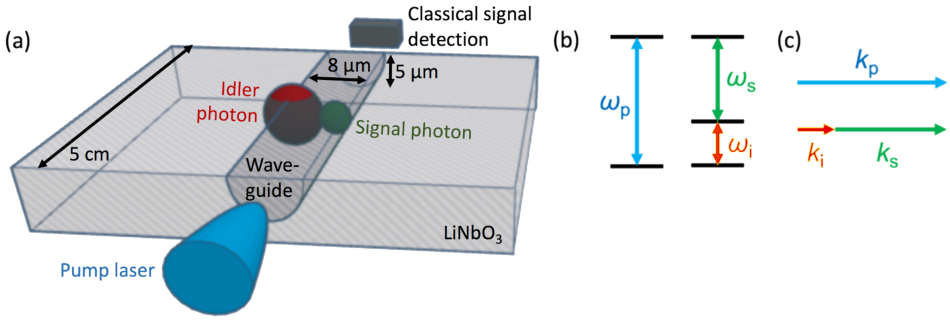

FIG. 1. (a) Scheme of our measurement approach. A continuous-wave pump laser is coupled to a $LiNbO_3$ waveguide and generates a photon pair consisting of a signal and an idler photon through spontaneous parametric down-conversion (SPDC). The generated photons are characterized by a spectrometer. Schemes of (b) energy conservation and (c) momentum conservation in SPDC.

possibly long interaction length in waveguide-based photon sources allows for high spectral resolution. Furthermore, this long interaction length ensures high photon-pair fluence even for low pump powers,[19,21] which is important for practical applications.

The photons generated in our waveguide are analyzed using a classical spectrometer based on an InGaAs detector, which is sensitive in the near-infrared (NIR) spectral range from 1000 nm to 1650 nm. Using this, we experimentally demonstrate the wide spectral tunability of waveguide SPDC. Furthermore, we show that the measurement of one of the paired photons in this well-accessible spectral range is sufficient to extract properties of the system at the wavelength of the other photon, which could be in the mid-infrared (MIR) spectral range above 2 μm wavelength. This capability provides the basis for implementation of SPDC spectroscopy on a chip.

We experimentally measure the intensity of the generated photon pairs for different pump wavelengths λ_p. To identify signals stemming from detector noise or background illumination, we also measure spectra with switched-off pump laser. The spectra obtained after subtracting these background spectra from the measured SPDC spectra are plotted in logarithmic scale in Fig. 2(a). We have performed comparable measurements at several different pump powers, which show linear dependence of the SPDC amplitude on the pump power, confirming that all presented spectra are in the low gain regime of single photon pairs. For pump wavelengths below 776 nm, we always find a characteristic spectral line stemming from phase-matched SPDC to the guided signal and idler in the fundamental mode of the waveguide as described above. At the upper limit, λ_p = 776 nm, the SPDC emission is degenerate, i.e., $\lambda_i = \lambda_s$. As the pump wavelength λ_p is getting smaller, the SPDC spectrum is also transformed, with signal and idler wavelengths spreading apart to ensure energy conservation. As the used spectrometer cannot detect radiation with wavelengths longer than 1650 nm, we are only able to register the short-wavelength signal photons. Nevertheless, using the known pump and signal wavelengths, we can calculate the wavelengths of the idler photons according to $\lambda_i = (1/\lambda_p - 1/\lambda_s)^{-1}$. For specific pump wavelengths, these deduced idler wavelengths are denoted in Fig. 2(a). For pump wavelengths below 765 nm, the generated idler wavelengths are above 2 μm.

The intensity of the spectral line of signal photons in the fundamental waveguide mode is proportional to the fluence of the emitted photon pairs. By calibrating the spectrometer with a classical cw-laser source at different signal wavelengths, we were able to determine the down-converted photon fluence for the pump power of 0.5 mW. The photon rate reaches 9×10^6 pairs/s at $\lambda_s = \lambda_i$ = 1552 nm and decreases to 3×10^6 pairs/s at λ_s = 1250 nm when only the signal photon branch

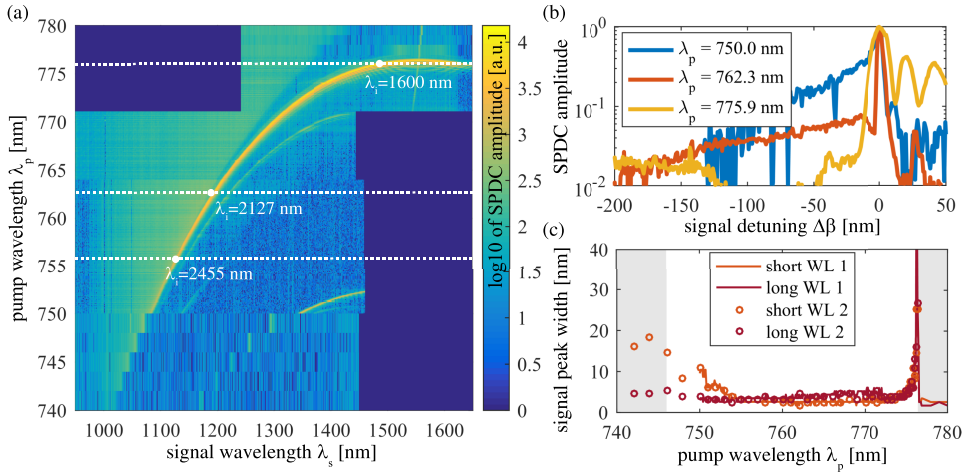

FIG. 2. (a) Measured intensity of photon pairs generated by SPDC in a $LiNbO_3$ waveguide in dependence on signal and pump wavelength. White circles indicate idler wavelengths λ_i for specific pairs of signal wavelengths λ_s and pump wavelengths λ_p. (b) Normalized SPDC spectra for three different pump wavelengths. (c) Half-widths of the measured spectral peaks towards long wavelengths (red solid lines/circles) and short wavelengths (orange solid lines/circles), where the solid lines and circles denote two independent measurement runs with two different spectral resolutions (WL 1 for higher resolution and WL 2 for lower resolution). The grey shading denotes pump wavelengths where no phase-matching between guided modes is expected.

is measured, in line with previous demonstrations of optical parametric generation in waveguides with higher pump powers.[19,21] Measuring only the signal photons is sufficient to estimate also the emitted idler fluence in the case of low loss for both wavelengths, as the same amount of signal and idler photons are generated, and also both photons reach the end of the waveguide. Higher losses for one of the involved photons would lead to significantly broadened SPDC spectra for non-degenerate SPDC,[17] which are not observed in the wavelength range where we measure the fluences.

In addition to the fundamental waveguide mode corresponding to the brightest dispersion curve, there are also fainter curves corresponding to the higher-order waveguide modes, where phase-matching is allowed for different sets of interacting wavelengths.[22] In the rest of this paper, we focus on the fundamental modes; however, higher-order modes can also be an interesting subject of study in respect to on-chip SPDC spectroscopy.[23] Furthermore, for signal wavelengths smaller than that in the prominent peak of the fundamental modes, we find a broad background, which we attribute to phase-matched SPDC to a guided fundamental mode at the signal wavelength and plane waves propagating in the lithium niobate substrate at the idler wavelength, similar to the Čerenkov configuration in second-harmonic generation.[24] The plane waves can have different propagation angles with respect to the waveguide and thus provide a continuum of modes to which the guided signal mode can be phase-matched.

We furthermore demonstrate that information about the waveguide properties in the MIR wavelength can be extracted from the measured spectra in the NIR. Spectra for three different pump wavelengths, denoted by the dashed lines in Fig. 2(a), are plotted in Fig. 2(b), where the wavelength axis is scaled relative to the wavelength of maximum SPDC. For a pump wavelength of 775.9 nm, close to the degeneracy wavelength, we find a broad maximum corresponding to the phase-matching of guided modes and a faint continuum at short wavelengths corresponding to phase-matching to plane waves. When the pump wavelength is decreased to 762.3 nm, the phase-matching peak of the guided modes is getting narrower and the continuum moves closer to this peak but is still separated by a clearly discernible minimum. For an even smaller pump wavelength of 750 nm, the distinct peak vanishes; instead, we observe a sharp cutoff of the generated continuum towards larger wavelengths.

To comprehensively analyze the transition between the regime of separated phase-matching of guided modes and plane waves and the regime where they are merged, we calculate the spectral half-width of the observed peaks, both in the directions towards long wavelengths and short wavelengths, respectively, and plot them in Fig. 2(c) in dependence on the pump wavelength. Close to the upper boundary for possible pump wavelengths, we find a large width in both directions. The phase-matching peak is getting narrower for smaller pump wavelengths but remains symmetric. The smallest measured half-widths are approximately 3 nm and are limited by the spectral resolution of the used spectrometer. If the pump wavelength is further decreased and in turn the difference in signal and idler wavelengths is increased, we find that the half-width towards smaller wavelengths is getting larger again, whereas the half-width towards larger wavelengths stays approximately constant. The onset of this asymmetric broadening corresponds to the wavelength in which the minimum separating SPDC to guided modes and SPDC to plane waves in the generated spectrum vanishes.

This transition denotes the cutoff of the guided mode at the idler wavelength. To support this interpretation, we carry out numerical simulations of the waveguide modes using the finite element method (FEM). Based on the known diffusion profiles of the Ti ions forming the core of the waveguide[25] and the wavelength-dependent refractive indices of LiNbO from Ref. 26, we calculate the propagation constants of the fundamental TM-polarized waveguide mode in a wide spectral range from 740 nm to 2600 nm. Above a wavelength of 2550 nm, no guided modes could be found. The obtained data is then used to determine wavelength combinations of λ_p, λ_s, and λ_i, for which energy conservation is fulfilled and the phase mismatch approaches zero, according to Eq. (1). Pump and signal combinations for which phase-matching can be achieved are plotted with the orange line in Fig. 3. For pump wavelengths below 748 nm, no phase-matching to guided modes could be identified, as guided modes above the corresponding idler wavelength of 2550 nm would be required, which do not exist. We compare the simulated phase-matching wavelengths with experimentally measured wavelength combinations, found by determining the signal wavelength of maximum SPDC intensity

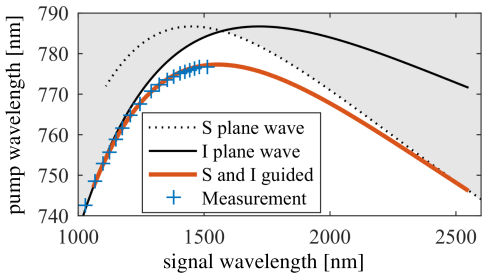

FIG. 3. Numerically calculated SPDC phase-matching curves of guided signal and idler modes (red solid line), guided signal mode and idler plane wave propagating parallel to the waveguide (solid black line), and guided idler mode and signal plane wave propagating parallel to the waveguide (dotted black line). The grey shading denotes regions where phase-matching of guided modes with plane waves propagating in other directions can take place. Measured phase-matching wavelengths for the case of signal and idler guided modes (blue crosses) are in excellent agreement with the measured spectral maxima, showing the overlapping phase-matching wavelengths to guided modes and plane waves further away from the degeneracy point.

for each pump wavelength. The measured values, denoted by the blue markers in Fig. 3, fit to the simulated curve very well.

Furthermore, with the black lines, we plot wavelength combinations in which phase-matching is achieved between one guided mode and a plane wave propagating in the lithium niobate crystal parallel to the waveguide. We consider both possibilities of either the signal or the idler being the plane wave, where solid (dashed) lines denote phase-matching of signal (idler) guided modes to idler (signal) plane waves. The grey shading denotes the continuum of wavelength combinations, where phase-matching of a guided mode to a plane wave propagating under an angle with respect to the waveguide is possible. The white region between the orange and black lines then corresponds to the spectral gap between guided modes and plane waves, which we observed in the experiment. For decreasing pump wavelength, this gap indeed is getting narrower. As exactly at the cutoff wavelength the propagation constants of the guided mode and of the parallel plane wave are the same, phase-matching to both can be fulfilled simultaneously, and the spectral gap closes entirely. This was observed in the measurement and is also found in the simulations.

To enable spectroscopic measurements using such waveguides, unknown substances outside the waveguide core have to be probed using the evanescent tails of the guided modes. Importantly, for measurements at the MIR idler wavelengths, only the idler mode should interact with the sample to be measured. This can be achieved using the very different mode sizes of the pump, signal, and idler. The idler mode at MIR wavelengths is much more delocalized than the other modes due to the longer wavelength. Thus, it can interact with an unknown substrate placed in close proximity to the waveguide. The complex refractive index experienced by the idler photon will be influenced by the substance in close proximity to the waveguide, whereas the signal and idler modes will not be affected. For the particular waveguide geometry utilized in our experiment, we propose a microfluidic channel close to the waveguide.[27] However, our general approach for waveguide-based spectroscopy can also be implemented in $LiNbO_3$ waveguides with other geometries, such as ridge waveguides,[28] which are expected to allow spectroscopy of gases and solids above the waveguide.

To assess this concept, we calculate the guided pump, signal, and idler eigenmodes for a system consisting of a lithium niobate waveguide and a parallel microfluidic channel with 1 μm × 1 μm cross section buried 6 μm below the substrate surface and 7 μm away from the waveguide center. The resulting mode profiles are shown in Fig. 4(a) for the pump, signal, and idler wavelengths of 750 nm, 1100 nm, and 2450 nm, respectively. We assume the microfluidic channel to be filled with a strongly absorbing high-index liquid with refractive index $n_l = 1.5 + 0.1i$, in which dispersion is neglected. It is clearly visible that the idler mode is influenced by the presence of the lossy channel, indicated by the white square in Fig. 4(a), whereas pump and signal modes are practically unaffected. Such placement of the microfluidic channel has minimal effect on the dispersion of the guided modes; hence, the waveguide characterization performed in this work is

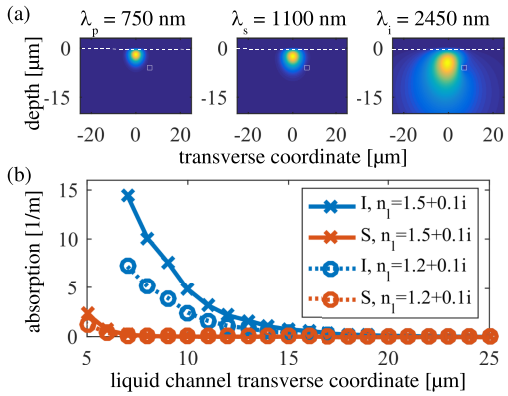

FIG. 4. (a) Intensity distributions of the pump (left), signal (middle), and idler (right) modes showing different mode sizes calculated for a lithium niobate waveguide and a parallel microfluidic channel indicated by a white square with 1 μm × 1 μm cross section buried 6 μm below the substrate surface and 7 μm away from the waveguide center. The white dashed lines mark the upper edge of the lithium niobate substrate. (b) Absorption coefficients for idler (blue) and signal (red) modes vs. the microfluidic channel transverse coordinate for high-index liquid (solid lines with crosses) and water-like liquid (dashed lines with circles).

expected to be useful for structures with microfluidic cavities. Nevertheless, further reference measurements with the microfluidic channel in place would be useful to increase the precision of SPDC spectroscopy.

Calculated mode absorption coefficients for signal and idler modes for different transverse positions of the microfluidic channel are plotted in Fig. 4(b) for the high-index liquid used in Fig. 4(a) and a liquid comparable to water with refractive index $n_l = 1.2 + 0.1$i. For distances closer than 7 μm, the idler mode is not guided; hence, no results can be obtained. For 7 μm distance, α_i is around 15 m^{-1} (7 m^{-1}) for the high-index liquid (water) case, which is about 70 times larger than the loss coefficient for the signal α_s and 4 orders of magnitude larger than the loss coefficient for the pump α_p (not shown). Although the absolute value of the idler mode losses decreases with increased distance of the microfluidic channel, the ratio α_i/α_s increases, leading to even better separation between effects caused by the signal and the idler.

Taking into account the differences in the loss coefficients and using the reference results obtained in this paper will allow separating the influence of the medium under test on the signal wave in future works. This way, spectroscopy of unknown substances in the MIR will become possible on a chip by relying only on classical spectral signal measurements in the NIR and reference measurements reported in this work. Increased sensitivity can potentially be achieved, similar to previous bulk optical implementations,[6,11,12] by using nonlinear interferometry between several SPDC sources integrated on a single chip. In this context, the interferometric stability of integrated photonics will become highly advantageous.

To summarize, we have evaluated the properties of a standard periodically poled waveguide in lithium niobate with respect to applications in on-chip SPDC spectroscopy. We experimentally demonstrated that strongly non-degenerate photon pairs with idler wavelength up to 2.5 μm can be generated, well outside the detection bandwidth of standard InGaAs detectors. To highlight the capability of obtaining information about the waveguide in the MIR spectral range without actually measuring there, we determined the cutoff of the guided mode at 2.4 μm wavelength. Our results fit well to the simulations of the phase-matching properties of the waveguide and lithium niobate chip. Furthermore, using simulations, we showed that these waveguides can also be used for spectroscopy of substances held in a microfluidic channel next to the waveguide. Importantly, our results show that this concept enables separating contributions of the idler, signal, and pump interaction with the analyte.

Hence, we can conclude that lithium niobate waveguides are a suitable platform to perform SPDC spectroscopy. Compared with previously demonstrated bulk optical approaches,[29] this on-chip system provides a compact solution and much higher SPDC efficiency reaching 9×10^6 pairs/s

for 0.5 mW of pump power. The available wavelength range can be further extended towards longer wavelengths by using optimized waveguide geometries.[30]

Australian Research Council (Nos. DP160100619 and DE180100070); Erasmus Mundus (No. NANOPHI 2013 5659/002-001); Alexander von Humboldt Foundation; Australia-Germany Joint Research Co-operation Scheme of Universities Australia; German Academic Exchange Service (Project No. ID 57218492); German Federal Ministry of Education and Research within the consortium 3Dsensation (No. FKZ 03ZZ0434); Carl-Zeiss-Foundation.

We thank Mirko Lobino, Leonid Krivitsky, Dmitry Kalashnikov, and Giuseppe Leo for useful discussions.

[1] B. H. Stuart, *Infrared Spectroscopy: Fundamentals and Applications*, Analytical Techniques in the Sciences (John Wiley & Sons, Ltd., Chichester, UK, 2004), pp. 1–224.
[2] T. P. Dougherty and E. J. Heilweil, "Dual-beam subpicosecond broadband infrared spectrometer," Opt. Lett. **19**, 129 (1994).
[3] E. J. Heilweil, "Ultrashort-pulse multichannel infrared spectroscopy using broadband frequency conversion in $LiIO_3$," Opt. Lett. **14**, 551 (1989).
[4] G. K. Kitaeva and A. N. Penin, "Spontaneous parametric down-conversion," J. Exp. Theor. Phys. Lett. **82**, 350–355 (2005).
[5] D. C. Burnham and D. L. Weinberg, "Observation of simultaneity in parametric production of optical photon pairs," Phys. Rev. Lett. **25**, 84–87 (1970).
[6] M. V. Chekhova and Z. Y. Ou, "Nonlinear interferometers in quantum optics," Adv. Opt. Photonics **8**, 104–155 (2016).
[7] A. L. Aleksandrovskii, G. I. Ershova, G. K. Kitaeva, S. P. Kulik, I. I. Naumova, and V. V. Tarasenko, "Dispersion of the refractive indices of LiNbO3:Mg and LiNbO3:Y crystals," Sov. J. Quantum Electron. **21**, 225 (1991).
[8] A. S. Solntsev, G. K. Kitaeva, I. I. Naumova, and A. N. Penin, "Measurement of the extraordinary refractive index dispersion in the MIR for Mg:Nd:LiNbO3 crystals by the use of quasi-phase-matching in a random 1D domain structure," Appl. Phys. B **99**, 197–201 (2010).
[9] G. K. Kitaeva, V. V. Tishkova, I. I. Naumova, A. N. Penin, C. H. Kang, and S. H. Tang, "Mapping of periodically poled crystals via spontaneous parametric down-conversion," Appl. Phys. B **81**, 645–650 (2005).
[10] A. S. Solntsev, G. K. Kitaeva, I. I. Naumova, and A. N. Penin, "Characterization of aperiodic domain structure in lithium niobate by spontaneous parametric down-conversion spectroscopy," Laser Phys. Lett. **12**, 095702 (2015).
[11] D. A. Kalashnikov, A. V. Paterova, S. P. Kulik, and L. A. Krivitsky, "Infrared spectroscopy with visible light," Nat. Photonics **10**, 98–101 (2016).
[12] A. Paterova, S. Lung, D. A. Kalashnikov, and L. A. Krivitsky, "Nonlinear infrared spectroscopy free from spectral selection," Sci. Rep. **7**, 42608 (2017).
[13] V. V. Kornienko, S. A. Germanskiy, G. K. Kitaeva, and A. N. Penin, "Generation of optical-terahertz biphoton pairs via spontaneous parametric down-conversion," Int. J. Quantum Inf. **12**, 1560023 (2014).
[14] V. V. Kornienko, G. K. Kitaeva, I. I. Naumova, A. N. Tuchak, A. N. Penin, and P. V. Yakunin, "Evaluating the spectral sensitivity of the nonlinear-optical terahertz wave radiation detecors via spontaneous parametric down-conversion spectra," Opt. Spectrosc. **116**, 520–528 (2014).
[15] S. Bogdanov, M. Y. Shalaginov, A. Boltasseva, and V. M. Shalaev, "Material platforms for integrated quantum photonics," Opt. Mater. Express **7**, 111–132 (2017).
[16] A. S. Solntsev and A. A. Sukhorukov, "Path-entangled photon sources on nonlinear chips," Rev. Phys. **2**, 19–31 (2017).
[17] M. Ravaro, E. Guillotel, M. L. Du, C. Manquest, X. Marcadet, S. Ducci, V. Berger, and G. Leo, "Nonlinear measurement of mid-infrared absorption in AlOx waveguides," Appl. Phys. Lett. **92**, 151111 (2008).
[18] E. L. Wooten, K. M. Kissa, A. Yi-Yan, E. J. Murphy, D. A. Lafaw, P. F. Hallemeier, D. Maack, D. V. Attanasio, D. J. Fritz, G. J. McBrien, and D. E. Bossi, "A review of lithium niobate modulators for fiber-optic communications systems," IEEE J. Sel. Top. Quantum Electron. **6**, 69–82 (2000).
[19] W. Sohler, H. Hu, R. Ricken, V. Quiring, C. Vannahme, H. Herrmann, D. Büchter, S. Reza, W. Grundkötter, S. Orlov, H. Suche, R. Nouroozi, and Y. Min, "Integrated optical devices in lithium niobate," Opt. Photonics News **19**, 24–31 (2008).
[20] A. S. Solntsev, F. Setzpfandt, A. S. Clark, C. W. Wu, M. J. Collins, C. Xiong, A. Schreiber, F. Katzschmann, F. Eilenberger, R. Schiek, W. Sohler, A. Mitchell, C. Silberhorn, B. J. Eggleton, T. Pertsch, A. A. Sukhorukov, D. N. Neshev, and Y. S. Kivshar, "Generation of nonclassical biphoton states through cascaded quantum walks on a nonlinear chip," Phys. Rev. X **4**, 031007 (2014).
[21] K. Gallo, M. De Micheli, and P. Baldi, "Parametric fluorescence in periodically poled LiNbO3 buried waveguides," Appl. Phys. Lett. **80**, 4492–4494 (2002).
[22] F. Setzpfandt, M. Falkner, T. Pertsch, W. Sohler, and R. Schiek, "Bandstructure measurement in nonlinear optical waveguide arrays," Appl. Phys. Lett. **102**, 081104 (2013).
[23] F. Setzpfandt, A. S. Solntsev, and A. A. Sukhorukov, "Nonlocal splitting of photons on a nonlinear chip," Opt. Lett. **41**, 5604–5607 (2016).
[24] M. Li, M. De Micheli, Q. He, and D. Ostrowsky, "Cerenkov configuration second harmonic generation in proton-exchanged lithium niobate guides," IEEE J. Quantum Electron. **26**, 1384–1393 (1990).
[25] G. P. Bava, I. Montrosset, W. Sohler, and H. Suche, "Numerical modeling of Ti:$LiNbO_3$ integrated optical parametric oscillators," IEEE J. Quantum Electron. **23**, 42 (1987).
[26] G. J. Edwards and M. Lawrence, "A temperature-dependent dispersion equation for congruently grown lithium niobate," Opt. Quantum Electron. **16**, 373–375 (1984).

[27] G. Bettella, "Integrated opto-microfluidic lab-on-a-chip in lithium niobate for droplet generation and sensing," Ph.D. thesis, University of Padua, 2016, see http://paduaresearch.cab.unipd.it/9576/.
[28] R. Geiss, S. Saravi, A. Sergeyev, S. Diziain, F. Setzpfandt, F. Schrempel, R. Grange, E.-B. Kley, A. Tünnermann, and T. Pertsch, "Fabrication of nanoscale lithium niobate waveguides for second-harmonic generation," Opt. Lett. **40**, 2715–2718 (2015).
[29] D. A. Kalashnikov, Z. Pan, A. I. Kuznetsov, and L. A. Krivitsky, "Quantum spectroscopy of plasmonic nanostructures," Phys. Rev. X **4**, 011049 (2014).
[30] Y. M. Sua, H. Fan, A. Shahverdi, J.-Y. Chen, and Y.-P. Huang, "Direct generation and detection of quantum correlated photons with 3.2 μm wavelength spacing," Sci. Rep. **7**, 17494 (2017).